

K-band Planar and Low-profile Fabry-Perot Cavity Antenna with a Coupled Strip-Slitline Feed Structure

Huy Hung Tran^{1,2} and Truong Khang Nguyen^{1,2,*}

¹Division of Computational Physics, Institute for Computational Science
Ton Duc Thang University, Ho Chi Minh City, Vietnam

²Faculty of Electrical & Electronics Engineering, Ton Duc Thang University, Ho Chi Minh City, Vietnam
tranhuyhung@tdt.edu.vn, *nguyentruongkhang@tdt.edu.vn

Abstract — In this paper, a design of a planar, low-profile, and high gain Fabry-Perot cavity antenna for K-band applications is presented. The antenna is consisted of a frequency selective surface (FSS) made of a circular hole array and a feeding structure made of a coupled strip-slitline. The FSS and the slitline both are lithographically patterned on a high permittivity substrate while the stripline is printed on top of a thin and low permittivity substrate. These two substrates are then closely appressed each other to form a planar structure. The measured results show that the proposed antenna has an impedance bandwidth of about 4% ($|S_{11}| \leq -10$ dB), a maximum gain of about 10.4 dBi, and a 3-dB gain bandwidth of approximately 2.9% at the resonance frequency of around 20.8 GHz. The antenna's compact, planar, and lightweight profile, i.e., approximately $4\lambda_0 \times 4\lambda_0 \times 0.24\lambda_0$ of a free-space wavelength at 21.0 GHz makes it promising for a small and efficient source in K-band applications.

Index Terms — Antennas, Fabry-Perot cavity, leaky-wave.

I. INTRODUCTION

In the last years, the idea of using a planar and low-profile Fabry-Perot (FP) cavity antenna for applications demanding easy and cost-effective fabrication have received significantly attention because of its number of attractive properties, such as low profile, high directivity, mechanical robustness, and capability of conformal deployment [1-7]. This kind of technique with the fully dielectric integration poses two main design challenges, particularly for high permittivity substrate in order for miniaturization, that are low radiation efficiency causing reduced antenna gain and narrow 3-dB gain/power bandwidth limiting the uses of antenna to wireless communication systems [8-10]. In addition, there have few papers considered on the common (available) bandwidth in a Fabry-Perot resonator antenna. The common bandwidth specification

is the overlapping frequency range between the 10-dB return loss bandwidth and the 3-dB gain bandwidth [11].

In this paper, a Fabry-Perot resonator cavity antenna satisfying planar, low profile, high gain, and moderate common bandwidth requirements is designed. The antenna is consisted of a frequency selective surface (FSS) made of a circular hole array and a coupled strip-slitline feed. The resonator is formed by the FSS and the slitline ground plane. In particular, the cavity resonance is efficiently excited by a coupling mechanism of a microstrip-substrate integrated waveguide transition and thus the high gain characteristic is obtained.

II. ANTENNA DESIGN AND MODELLING THE STRUCTURE

The geometry of the proposed antenna is depicted in Fig. 1 with front and top views. The cavity was made of a Taconic substrate whose dielectric constant and loss tangent are $\epsilon_{r1} = 10.2$ and $\tan\delta = 0.0035$, respectively. A leaky-wave open-ended narrow slitline of width W_{slit} and a very thin metallic FSS were lithographically patterned both on the top side and bottom side of the substrate. Therefore, the cavity is formed by the FSS sheet and the ground plane of the slitline and its resonance length is determined by the substrate thickness of H . The FSS is a bi-periodic 9×9 array of circular holes whose hole diameter and periodicity are D and P , respectively. In order to excite the cavity resonance, a slit-coupled feeding technique with a simple stripline is used. The stripline is printed on a thin and very low dielectric constant RT/Duroid 5880 substrate whose thickness is denoted by T and dielectric constant is $\epsilon_{r2} = 2.2$. The length and width of the stripline are designated by L_{strip} and W_{strip} , respectively. The overall dimension of the proposed antenna is $A \times A \times (H+T)$ mm³. The optimized parameters of the antenna were as follows: $A = 56$ mm, $H = 3.175$ mm, $T = 0.254$ mm, $D = 3.8$ mm, $P = 5.2$ mm, $L_{strip} = 31.1$ mm, $W_{strip} = 0.9$ mm, and $W_{slit} = 0.3$ mm.

All electromagnetic simulation is performed using CST Microwave Studio which is based on the finite-integration time-domain (FIT) technique [12]. A unit cell model was first employed to evaluate the reflection characteristics of the cavity which is formed by FSS and the ground plane of the open-ended slitline. In this model, a two-Floquet-ports model with magnetic and electric boundary conditions enforced along $\pm x$ and $\pm y$. This allows to simulate a normal mode propagation for the waveguide configuration. Frequency-domain solver with tetrahedral meshes is used in this simulation step. Figure 2 shows that the FP cavity mode is excited when S11 presents an 180° reflection phase. The predicted resonance frequency of the FP cavity is approximately 21.3 GHz. At this resonance frequency, the hole is efficiently excited, and the field leaked through the hole, which contributes to the antenna directivity, is maximized.

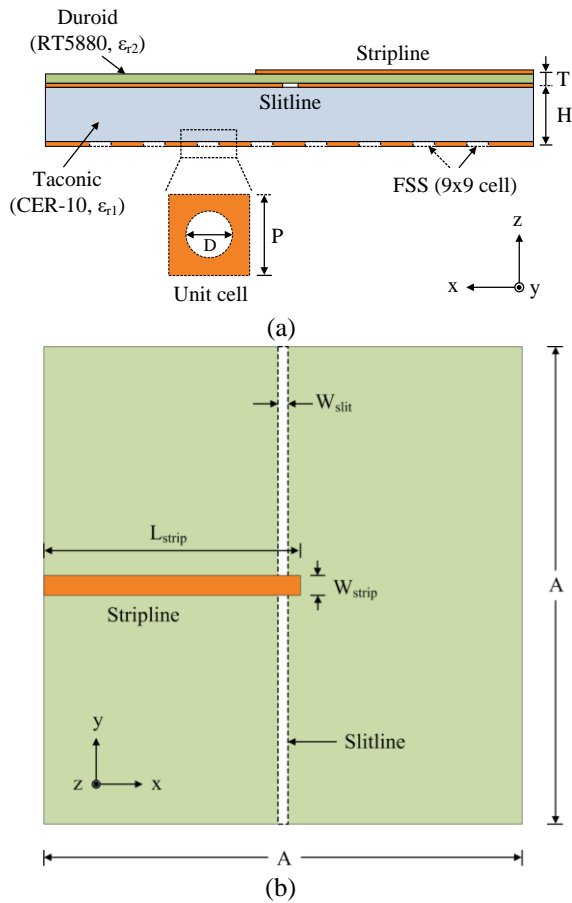


Fig. 1. (a) Side and (b) top views of the proposed FPC antenna.

II. ANTENNA CHARACTERISTICS

The antenna characteristic is investigated and optimized by using a full three-dimensional structure finite size and real shape. In this model, principally

open with some added space boundaries are used in order to accurately calculate the antenna radiation patterns. In this simulation, transient time-domain solver and a hexahedral mesh scheme is used. This approach saves the computation time and resources while allows to monitor the radiation performance of the antenna in a broad frequency range within one simulation run.

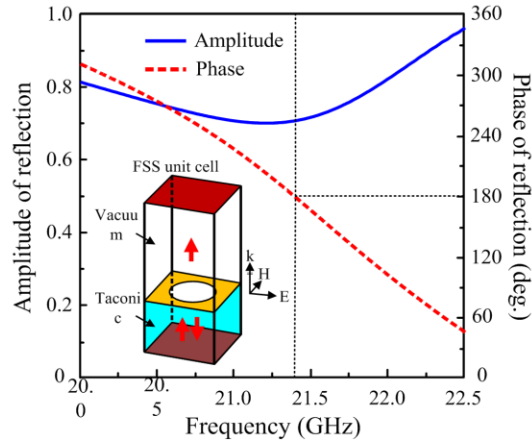


Fig. 2. Reflection characteristic of the FP cavity in the unit cell model (inset).

Figures 3 (a)-(c) shows the boresight gain characteristic with respect to the design parameters such as substrate cavity dimensions and number of hole in the FSS array, respectively. In general, the increases in the thickness and the lateral size of the substrate lead to a linear shift in the frequency. Besides, the boresight gain profile of the antenna in the variation of the substrate lateral size was altered along with the frequency shift, which behaved differently compared with the cases having substrate thickness variation. This behavior is attributed to the truncation effect resulting from the finite lateral dimension of the substrate [13]. The number of holes also affected the effective permittivity of the cavity. As seen in Fig. 3 (c), when the number of holes in the array changed from 1×1 to 2×2 to 3×3 to 4×4 , that is, while fixing the lateral size A , the gain profile changed, particularly in the lower frequency region, and the frequency occurring maximum gain slightly decreased. In general, more number of holes in the array resulted in a larger effective aperture and thus enhancing the antenna gain. From these results, it can be seen that the Taconic substrate dimensions contributed to the effective permittivity of the cavity, and consequently determined the resonance condition to obtain maximum boresight gain of the antenna. Therefore, such changes on these parameters caused an out-of-resonance condition in both the cavity and the FSS, thereby reducing the beam collimation or the antenna boresight gain.

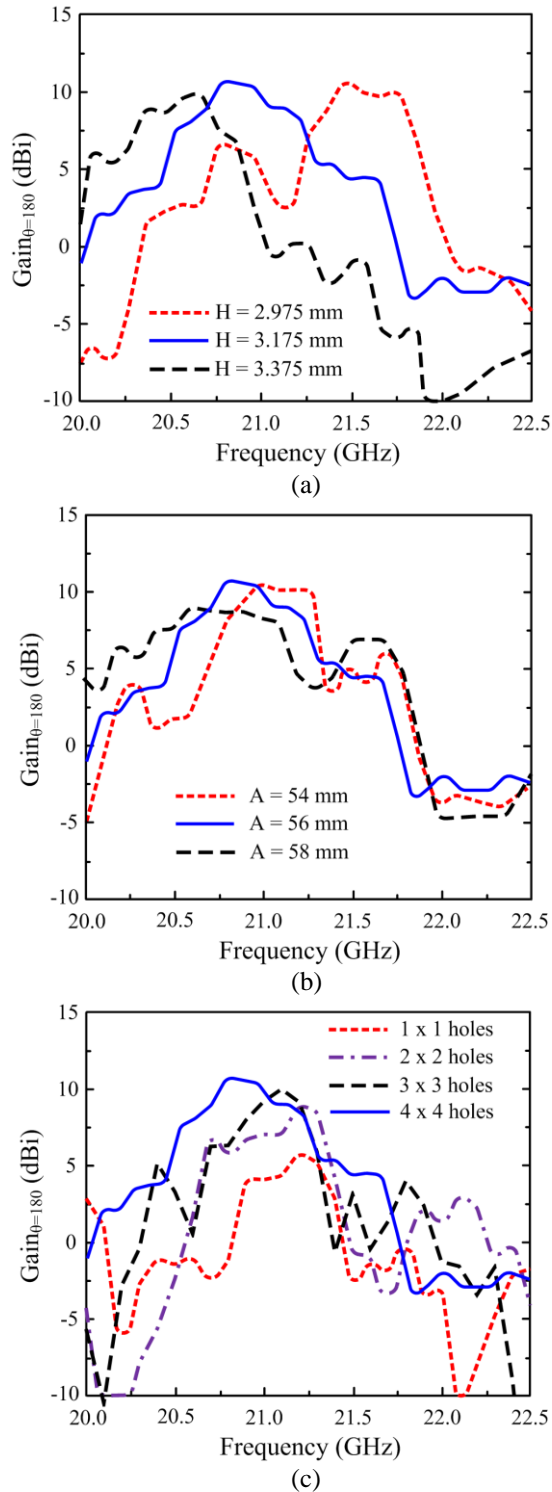


Fig. 3. Antenna gain characteristics with respect to: (a) Taconic substrate thickness H , (b) lateral size A for both substrates, and (c) number of circular holes in the array.

The electric field distributions along the stripline (xz -plane) and along the leaky-wave slitline (yz -plane) have been calculated and described in Fig. 4. The results show that, at the resonance frequency of 20.8 GHz, radiation is minimized at the edges of the substrate and in the back side of the antenna. This observation, thereby, verifies the directional beam pattern of the proposed antenna. In other words, this demonstrates that the Fabry-Perot cavity made of Taconic substrate the FSS hole array and was effectively excited by the slit-coupled feeding structure while avoiding unwanted back-side-radiation across a broad frequency range.

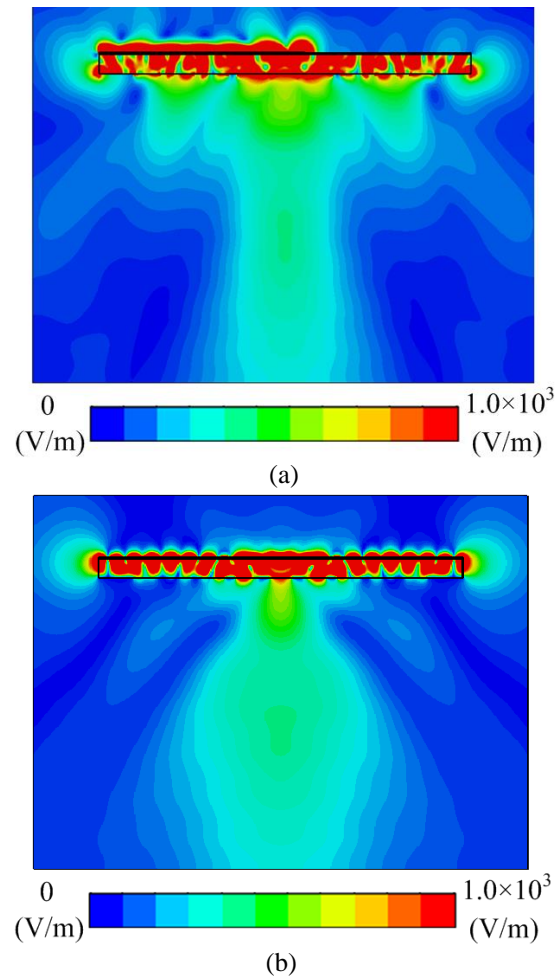


Fig. 4. E-field distributions at 20.8 GHz in: (a) xz -plane and (b) yz -plane of the optimized antenna.

III. MEASUREMENT RESULTS

The photograph of the fabricated antenna is shown in Fig. 5 with top, bottom, and side views. Figure 6 shows the results of $|S_{11}|$ and boresight gain as a

function of frequency in a comparison between the simulation and measurement. The E8362C Agilent PNA Microwave Network Analyzer was used to measure the $|S_{11}|$ of the fabricated antenna. Generally, the measured $|S_{11}|$ and boresight gain were close to the simulated ones. The approximate 0.1 GHz downward shifts of the measured $|S_{11}|$ and boresight gain in comparison to the simulated ones were observed which were mainly due to the tolerance of the dielectric constant of the Taconic substrate, i.e., specified as 10.2 ± 0.5 , and the tiny gap between the two closely appressed substrates, i.e., Duroid and Taconic substrates. The measured impedance bandwidth for $|S_{11}| \leq -10$ dB was about 0.9 GHz (20.6–21.5 GHz), which is approximately 4% fractional bandwidth at the 21.0 GHz center frequency. The antenna produced a measured maximum gain of about 10.4 dBi at 20.8 GHz. The achieved 3-dB gain bandwidth of the measured antenna was about 0.6 GHz, i.e., from 20.5 GHz to 21.1 GHz, corresponding to approximately 2.9% at the center frequency of 20.8 GHz. From these results, the proposed antenna obtained an approximate of 2.4% (20.6–21.1 GHz) common (available) bandwidth which is improved compared to the previously reported [10].

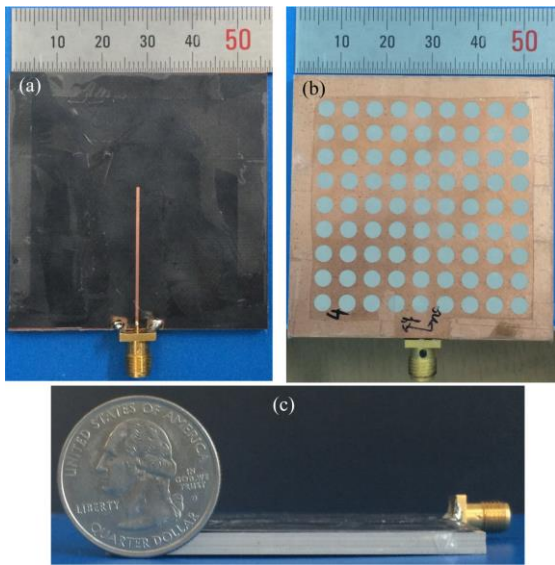


Fig. 5. Photographs of the fabricated antenna with: (a) top, (b) bottom, and (c) side views.

Figure 7 plots the measured radiation patterns in two principle planes at three selected frequencies within the 3-dB gain bandwidth of the antenna. The yz -plane presented symmetry radiation patterns whereas the xz -plane presented asymmetry radiation pattern which is due to the feeding configuration. The main beams in the xz -plane became narrower remarkably as increasing the frequency, whereas those in the yz -plane were almost

the yz -plane indicates the traveling-wave effect of the open-ended slitline. Generally, it is obvious that the unchanged. Such stability of the main beam pattern in proposed antenna produced good radiation characteristics that are good beam collimation, clean main beam, and low side lobes levels.

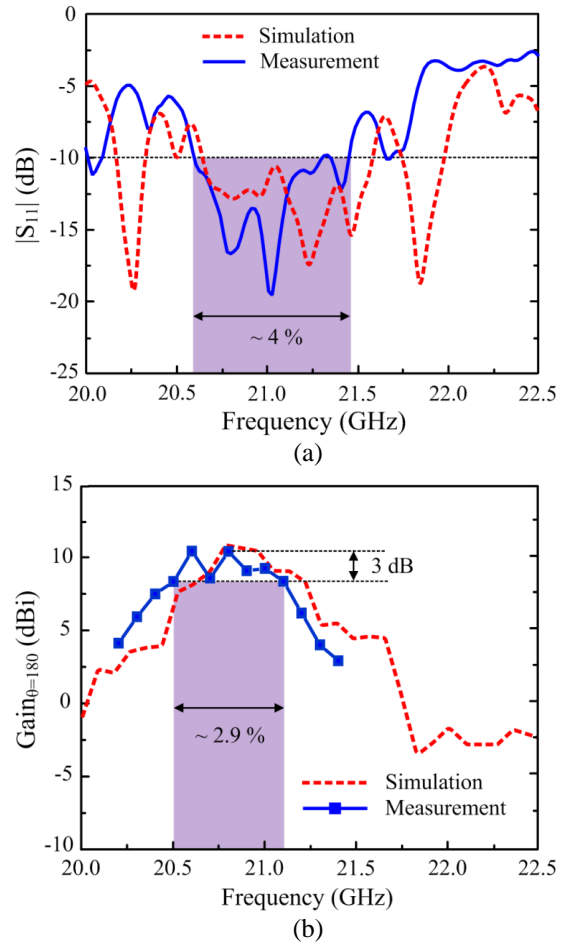
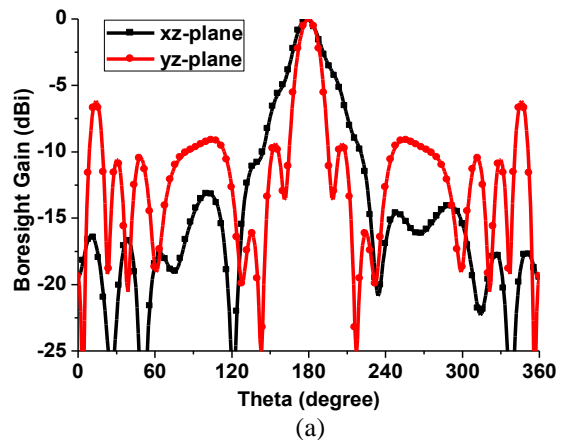


Fig. 6. (a) Reflection coefficient $|S_{11}|$, and (b) boresight gain of the proposed antenna.



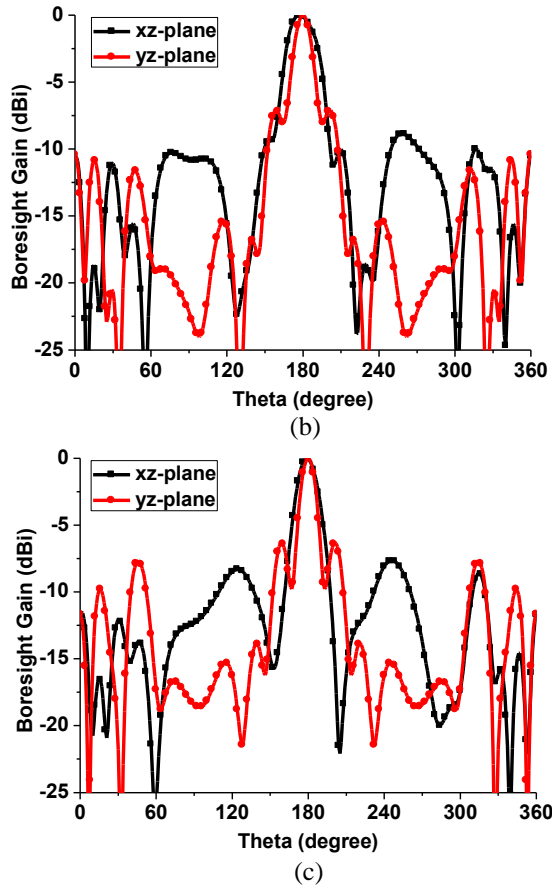


Fig. 7. Measured radiation patterns of the proposed antenna at different frequencies: (a) 20.6 GHz, (b) 20.8 GHz, and (c) 21.0 GHz.

VI. CONCLUSION

In this paper, we present a Fabry-Perot cavity antenna for *K*-band applications. The antenna presents its planar, low-profile, high gain, and improved common bandwidth characteristics. The results indicate that the strip-coupled-slitline feeding structure effectively excited the resonance of the substrate cavity. The antenna obtained good radiation patterns over the entire the 3-dB gain frequency bandwidth. In particular, the common (available) bandwidth is improved. The study shows that the performance of such planar Fabry-Perot resonator antenna can be improved by properly designing the feeding structure besides carefully modifying and optimizing of the FSS geometry [14].

ACKNOWLEDGMENT

This research is funded by Vietnam National Foundation for Science and Technology Development (NAFOSTED) under grant number 103.05-2016.37.

REFERENCES

- [1] G. V. Trentini, "Partially reflecting sheet array," *IRE Trans. Antenn. Propagat.*, vol. 4, pp. 666-671, 1956.
- [2] R. E. Collin and F. J. Zucker, *Antenna Theory*. New York, Wiley, 1969.
- [3] D. R. Jackson and N. Alexopoulos, "Gain enhancement methods for printed circuits antennas," *IEEE Trans. Antenn. Propagat.*, vol. 33 pp. 976-987, 1985.
- [4] A. P. Feresidis and J. C. Vardaxoglou, "High-gain planar antenna using optimized partially reflective surfaces," *IEE Proc. Microw. Antenn. Propagat.*, vol. 148, pp. 345-350, 2001.
- [5] H. Boutayeb, K. Mahdjoubi, A.-C. Tarot, and T. A. Denidni, "Directivity of an antenna embedded inside a Fabry-Perot cavity: Analysis and design," *Microw. Opt. Technol. Lett.*, vol. 48, pp. 12-17, 2006.
- [6] Y. Zhang, W. Yu, and W. Li, "Study on Fabry-Pérot antennas using dipole exciters," *Applied Computational Electromag. Soc. J.*, vol. 29 no. 12, pp. 1112-1116, 2014.
- [7] G. Di Massa, S. Costanzo, and H. O. Moreno, "Planar Fabry-Perot directive antenna: A simplified analysis by equivalent circuit approach," *J. Electromagn. Waves Appl.*, vol. 29, no. 2, pp. 261-274, 2015.
- [8] Y. Sun, Z. N. Chen, Y. Zhang, H. Chen, and T. S. P. See, "Subwave-length substrate-integrated Fabry-Pérot cavity antennas using artificial magnetic conductor," *IEEE Trans. Antenn. Propagat.*, vol. 60, pp. 30-35, 2012.
- [9] J. Ju, D. Kim, and J. Choi, "Fabry-Perot cavity antenna with lateral metallic walls for WiBro base station applications," *Electron. Lett.*, vol. 45, pp. 141-142, 2009.
- [10] T. K. Nguyen and I. Park, "Design of a substrate-integrated Fabry-Perot cavity antenna for *K*-band applications," *Int. J. Antenn. Propagat.*, 373801, pp. 1-12, 2015.
- [11] T. K. Nguyen and I. Park, "Design of a low-profile, high-gain Fabry-Perot cavity antenna for *Ku*-band applications," *J. Electromagn. Eng. Sci.*, vol. 14 pp. 306-313, 2014.
- [12] CST Microwave Studio, CST GmbH, 2016. <http://www.cst.com>
- [13] T. K. Nguyen, B. Q. Ta, and I. Park, "Design of a planar, high-gain, substrate-integrated Fabry-Perot cavity antenna at terahertz frequency," *Current Applied Phys.*, vol. 15, no. 9, pp. 1047-1053, 2015.
- [14] L. Zhou, X. Chen, and X. Duan, "High gain

Fabry-Perot cavity antenna with phase shifting surface,” *IEEE/ACES Int. Conf. on Wireless Infor. Tech. and Sys. (ICWITS) and Applied Comput. Electromag. (ACES)*, Hawaii, USA, 2016.



Huy Hung Tran received the B.S. degree in Electronics and Telecommunications from Hanoi University of Science and Technology, Hanoi, Vietnam in 2013, and the M.S. degree in the Department of Electrical and Computer Engineering, Ajou University, Suwon, Korea in 2015. His research is focused on wideband circularly polarized, and metamaterial for next generation wireless communication systems.



Truong Khang Nguyen received the B.S. degree in Computational Physics from the University of Science, Vietnam National University, Ho Chi Minh City, and the M.S. and Ph.D. degrees in Electrical and Computer Engineering from Ajou University in Suwon, Korea. He is currently Head of Division of Computational Physics, Institute for Computational Science & Faculty of Electrical-Electronics Engineering, Ton Duc Thang University in Ho Chi Minh City, Vietnam. He has authored and co-authored over 60 peer-reviewed international journal and conference papers. He has written one book chapter in the area of terahertz antenna and filed one patent on THz stripline antenna. His current research interests include the design and analysis of microwave, millimeter-wave, terahertz wave, and nano-structured antennas.